**International Journal of Advanced Research in Physical Science (IJARPS)**
*Volume 11, Issue 06, 2024, PP 1-17*
*ISSN (Online)-2349-7882*
*www.arcjournals.org*

# To Question about Main Principles and Criteria of Critical Processes and Phenomena

**Petro P. Trokhimchuck***

*Anatoliy Svidzinskiy Department of Theoretical and Computer Physics, Lesya Ukrayinka Volyn' National University, 13 Voly Avenue, 43025, Lutsk, Ukraine.*

***Corresponding Author:** ***Petro P. Trokhimchuck,*** *Anatoliy Svidzinskiy Department of Theoretical and Computer Physics, Lesya Ukrayinka Volyn' National University, 13 Voly Avenue, 43025, Lutsk, Ukraine.*

**Abstract:** *Main peculiarities of formulation main principles and criteria of critical processes and phenomena are discussed. Thermonuclear fusion, phenomena of Nonlinear and Relaxed Optics, physics of shock processes were selected for analysis. It is shown that the formation of these criteria is closely related to the problem of saturation of the excitation of the corresponding reactants of the system. At the same time, the principles can be thermodynamic, concentration, and systemic in nature. A detailed analysis of the Lawson criterion and the corresponding principles of Relaxed Optics was carried out. The prospects for the development of these studies were considered.*

**Keywords:** *critical processes, Relaxed Optics, Lawson criterion, Relaxed Optics, cascade processes, shock processes, coherent zone.*

## 1. INTRODUCTION

The formulation of principles and criteria for critical processes and phenomena is a rather complex problem. It is often difficult to identify any comprehensive features there [1 – 36]. In this work, we will note the most significant general features that are characteristic of almost all critical processes. Here, by critical processes, we mean processes that are usually accompanied by phase transformations of substances during various types of interaction.

The general characteristics of these processes include reaching a certain threshold of their generation, maintaining a stationary regime in the case of long-term processes (for example, thermonuclear fusion [3 – 5], operation of nuclear reactors [1, 2], etc.); the problem of excitation saturation for various phase transformations (phase transitions, effects of Nonlinear and Relaxed Optics, etc.) [11 – 13, 23 – 25, 27 – 29, 34].

It should be noted that the problem of choosing essential parameters plays an important role. Thus, in hydrodynamics similarity criteria were developed, which are characterized by the corresponding numbers (Reynolds, Prandtl, Rayleigh, Nusselt and their magnetic counterparts, etc.) [6 – 9, 24, 36].

Two Wigner-Vigner theorems of the theory of nuclear reactors are analyzed [1]. It is shown that these criteria are necessary, but in some cases not sufficient conditions for the stable operation of reactors.

The main features of the construction of the Lawson criterion [3] and Schönberg -Chandrasekhar evolutionary limit [4, 5] for thermonuclear reactions are considered [3].

The analogy between phase transitions of the second kind and nonlinear optical phenomena is analyzed. The expediency of transition in a number of cases when describing non-linear optical phenomena to physico-chemical representations is shown, as they are, as a rule, more universal.

The problem of similarity in hydrodynamics is considered. In particular, the Rayleigh-Chandrasekhar theory of the Thomson-Bernard effect is analyzed [6 – 9, 24, 36].

Selected criteria for description and management of Relaxed Optical processes. In particular, the conditions of laser doping of antimonide and indium arsenide with ruby laser pulses were analyzed. Criteria for effective laser annealing of ion-implanted layers of semiconductor materials have also been developed (laser radiation must be absorbed by ion-implanted layers only) [23 – 25, 34].

The criteria for cascade laser-induced phase transformations in germanium and silicon [15, 16, 23, 26] are given. It is shown how it can be used in the formation of laser-induced surface structures [23].

The criteria that should be used for laser-induced optical breakdown of the medium are analyzed. In particular, cascade processes are considered: diffraction stratification of focused laser radiation, generation of Cherenkov radiation and its interference [35, 28, 29, 34].

The criteria for the relationship between acoustic and electromagnetic shock processes are derived, as well as the criteria corresponding to their separate implementation [32, 33].

The idea of the unification of these methods and their wider application in modern physics is expressed.

## 2. MAIN RESULTS

### 2.1. Nuclear Reactors and Critical Processes

The main process that leads to the production of energy in nuclear reactors is the chain reaction of the decay of nuclei with the release of neutrons. The chain reaction will be self-sustained if the average number of reaction carriers that arise when one initial carrier interacts with the fuel and in turn interact with the fuel is at least one. This number is called the criticality coefficient and is denoted by the symbol C. The criticality coefficient gives the ratio of the number of carriers of one generation to the number of carriers of the previous generation. The value of this quantity depends on the size and shape of the reactor, so this quantity is extensive [1].

If there were $N_1$ carriers in the first generation, then in the nth generation the number of carriers is equal to [1]

$$N_n = N_1 C^{n-1}. \quad (1)$$

For $C = 1$, we have a critical system, $C > 1$ - a supercritical system, and with $C < 1$ - a subcritical system. Formula (1) can be written in the form of a differential equation, if you enter the life time of one generation l. This time can be defined as the average time between adjacent generations. Then the time between the first and nth generations is equal to $t = (n - 1)l$. Substituting into formula (1) $t/l = n - 1$, we have

$$N(t) = N_1 C^{t/l} \quad (1\ a)$$

or

$$\frac{1}{N}\frac{dN}{dt} = \frac{\ln C}{l}. \quad (1\ b)$$

For reactors $C \sim 1$, therefore $\ln C = C - 1$. In this case, main kinetic equation has next kind

$$\frac{dN}{dt} = \frac{C-1}{l} N. \quad (1\ c)$$

In the problem of uranium nuclear reactors and corresponding bombs, it is necessary to distinguish stationary and quasi-stationary, as well as pulsed processes. Moreover, all the main processes of energy release have a cascade nature. In the reactor, they need to be slowed down a bit in order to obtain a stationary or quasi-stationary mode of operation, while in bombs it is necessary to highlight the moment when the energy is released, roughly speaking, in a pulse mode, which leads to an explosion. The technical implementation and calculation methods of such regimes differ significantly.

Criticality is the normal operating state of a nuclear reactor in which the nuclear fuel sustains a fission chain reaction [1]. A reactor reaches criticality (and is considered critical) when each fission releases enough neutrons to sustain the current chain of nuclear reactions.

Let us now consider the conditions of criticality in nuclear reactors. Let's start with simpler ones - homogeneous nuclear reactors without a reflector [1]. The theory of a homogeneous reactor without a reactor can be roughly reduced to the theory of neutron propagation in infinite media. Therefore, the spatial distribution of neutrons and the criticality coefficient in a reactor of this type are internal characteristics of the environment, that is, they depend on the properties of materials and their physical and chemical structure. Even in reactors with a reflector at sufficiently large distances from the surface of the distribution between the active zone and the reflector, a distribution characteristic for reactors without a reflector is established. That is why the reactor theory without a reactor is also called the asymptotic theory for any other reactor theory [1].

In general, there are two criticality factors: static and dynamic. Static coefficient is important for reactors, dynamic coefficient for bombs. Therefore, in the future, we will consider only the static criticality coefficient.

This theory is based on two theorems: the first theorem is based on the distribution of neutrons, and the second on the probability of avoiding losses in a homogeneous reactor.

If the reactor is in a critical state, then its criticality coefficient is equal to unity, and the neutron flux distribution is stationary To calculate the criticality coefficient and neutron flow distribution in a non-critical reactor, we will reduce it to a critical one as follows. A real non-critical reactor, in which the number of neutrons released in one act of fission is equal to $\nu$, is replaced by a model reactor that is identical to the real one, but has a criticality number $\nu'$, absorbed so that the selected reactor is exactly critical. If the real reactor is subcritical, then $\nu'$ must be greater than $\nu$, and thus $\nu'/\nu > 1$.

The criticality coefficient for all cases is proportional to the number of neutrons released in one act of fission. From the condition of heterogeneity of the medium, we have that the probability of avoiding losses $P$ and the fraction of neutrons $f$ used in the active medium does not change, and the following conditions must be fulfilled [1]:

in real reactor

$$C = \frac{\nu}{1+\alpha} P, \tag{2 a}$$

and in model reactor

$$C' = \frac{\nu'}{1+\alpha} P. \tag{2 b}$$

Therefore,

$$C = \frac{\nu}{\nu'}. \tag{2 c}$$

Where $\alpha = \frac{\sigma_c}{\sigma_f}$, and $\sigma_c$ is radiation capture cross section, $\sigma_f$ – radiation division cross section.

Thus, the criticality coefficient of a non-critical reactor can be found by calculating the value of m', which makes the model reactor exactly critical, and then using formula (1).

Let us present the main theorems of the theory of reactors.

The first basic theorem of reactor theory can be formulated as follows.

In the function $\Phi(x, E)$, which describes the stationary distribution of neutrons in a critical reactor without a reflector, the variables $x$ and $E$ are separated:

$$\Phi(x, E) = \varphi(E)\psi(x), \tag{3}$$

the spatial distribution of $\psi(x)$) is the basic solution of the wave equation

$$\Delta\psi(x) + B^2\psi(x) = 0, \tag{4}$$

that is, such a solution, which is positive for the entire reactor and is equal to zero on the extrapolated boundary.

For those cases when the theory of age is unsuitable, the method of empirical deceleration kernels is used.

Further, we postulate that the power of the thermal neutron source is given by the following expression

$$S_t(x) = \eta\Sigma_a(u)p \int K(x.x')\,\Phi_t(x')dx'. \tag{5}$$

Where $\eta$ is the number of fission neutrons generated by one absorbed neutron, $\Sigma_a$ – thermal neutron scattering cross section.

However, for an infinite homogeneous medium $K(x,x') = K(x-x')$. It follows from this that the equation is true for a thermal neutron reactor

$$D\Delta\Phi_t - \Sigma_a\Phi_t + k\Sigma_a \int K(x.x')\,\Phi_t(x')dx' = 0, \tag{6}$$

Where $D$ is diffusion coefficient of thermal neutrons, $k = \frac{\eta\Sigma_a(u)p}{\Sigma_a}$. The integral is taken over the entire reactor. Only thermal neutrons are considered here.

As a function of one variable, the kernel $K(x,x') = K(x-x')$ can be obtained by both theoretical and experimental methods.

Further, we assume that the integral in (6) can be extended to the entire domain and that the kernel depends only on $|x-x'|$.

It is easy to see that the solution of equation (6) $\Phi_t(x)$ is also a solution of equation $\Delta\Phi_t + B^2\Phi_t = 0$, if the next critical condition is fulfilled [1]

$$\frac{k\boldsymbol{K}(B)}{1+L^2B^2} = 1, \tag{7}$$

where $\boldsymbol{K}(B)$ is the Fourier image of a function $K(r)$, defined by formula (8), L is diffusion path length of thermal neutrons [1],

$$\boldsymbol{K}(B) = \int_0^\infty K(r)\, 4\pi r B^{-1}\sin Br dr. \tag{8}$$

The proof of this statement is based on the following fact: if ψ(x) satisfies the wave equation (4) and $\boldsymbol{K}$ is an isotropic kernel that depends only on the distance $|x-x'|$, i.e. if $K(x,x') = K(x-x')$, than

$$\int dx'\ K(x,x')\psi(x') = \boldsymbol{K}(B)\psi(x). \tag{9}$$

The consequence of this theorem is the fact that if $\Phi_t$ = ψ is substituted in (6), then all terms of this equation will be proportional to ψ and this factor can be neglected. The transformed equation is equation (7).

For a thermal neutron reactor, the theorem expressed through formulas (8) and (9) can also be formulated as follows: the probability of avoiding losses in a homogeneous reactor without a reflector is the Fourier image of the deceleration kernel.

It should be noted, that from a mathematical point of view, these two theorems are equivalent to the accuracy of the mathematical representation (differential or integral equations). In each specific case, you need to choose a method that allows you to solve the corresponding problem more easily. However, methods based on the first theorem are more common [1].

In general, these methods are the basis for the calculation of all reactor exceptions: starting with space and ship reactors and ending with nuclear power plants [2].

### 2.2. Thermonuclear Reaction and Lawson Criterium

Calculations of the power balance in thermonuclear reactors operating under various idealized conditions are given by Lawson [3].Two classes of reactors are considered: first, self-sustaining systems in which the charged reaction products are trapped and, secondly, pulsed systems in which the charged reaction products escape so that energy must be supplied continuously during the pulse. It is found that not only must the temperature be sufficiently high, but also the reaction must be sustained long enough for a definite fraction of the fuel to be burnt.

Main thermonuclear reaction are reactions between hydrogen isotopes: deuterium – deuterium, tritium – deuterium, Thes reaction have little crossectins $\sim 10^{-2}$ barns [3].

The energy relased per unit time and volume by thermonuclear reactions in a hot gas is given by

$$P_{reac} = n_1 n_2 \overline{v\sigma}(T)E. \tag{10}$$

Where $n_1$ and $n_2$are the number densties of the nuclej of thr first and second kinds, and $\overline{v\sigma}(T)$ is the product of the relative velocities of the nuclei and the reaction cross-section averaged over the Maxvellian velocity distribution corresponding to the temperature $T$, and $E$ is the energy released by one reaction.

For D – D reactiuon this formula may be represented as

$$P_{reac} = \frac{1}{2}n^2\overline{v\sigma}(T)E. \tag{11}$$

Energy can be lost from the hot gas in two ways, by radiation and by conduction. The power radiated per unite voloume in hydrogen is given as [3]

$$P_B = 1.4 \cdot 10^{-34} n^2 T^{1/2} \text{watts} \cdot cm^{-3}. \quad (11\ a)$$

Let us give an example of systems in which Reaction Products are retained. The orders of magnitude involved, the slowing down range of bthe charged reaction products in a gas at $10^8$ degrees and $10^4$ atmospheres pressure $\left(n = 3 \cdot 10^{17}\ {nnuclei}/{cm^3}\right)$ is on the order of kilometre. The range of neutrons is hundreds of kilometres [3].

In astrophysics, as a rule, stationary processes take place. This is especially true for stars that are on the main sequence of the Hertzsprung-Ressel diagram [4]. The life time of the stars on this diagram, depending on their spectral class, lasts from several million years to 100 million years. The stay of the star on the main sequence lasts until its nuclear fuel - hydrogen - is exhausted in its superstructure. More precisely, until, as established by M. Schönberg and S. Chandrasekhar [5], a helium nucleus with a mass of 10-20 percent of the mass of the Sun is formed in the center of the star.

The time it takes for a star to reach the Schönberg -Chandrasekhar evolutionary limit (that is, the time it spends on the leading sequence of the Hertzsprung-Ressel diagram) is estimated by the formula [4, 5]:

$$t_{LS} \sim \frac{M}{L} \cong 10^{10} \left(\frac{M_G}{M}\right)^{-2.5} years. \quad (12)$$

Where $M$ - the mass of the star in the masses of the Sun $M_G$, $L$ - the luminosity of the star in the luminosities of the Sun. Here it is taken into account that the luminosity of the star is $L \sim M^{-3.5}$ [] and that the reserves of thermonuclear energy are proportional to the total mass of the star. The final stage of this evolution is the formation of a red giant or supergiant [4].

As the hydrogen content in the star's core gradually decreases, the opacity coefficient of the core substance decreases [4]. This leads to a continuous restructuring of the star and, starting from a certain moment, such restructuring is accompanied by a compression of the core. Part of the potential energy the core, which is in the stage of gravitational compression, turns into heat, so the temperature in the core increases. It also grows in the layer that directly surrounds the stellar core. Since hydrogen in the nucleus at a critical temperature produces helium as a result of fusion, the mass of the helium nucleus increases. This leads to a local increase in the force of gravity, further compression of the core and an additional increase in temperature in it. The duration of this process is very short - only about one percent of the previous evolutionary stage of the main sequence. As a result, convective currents arise that inflate the initial envelope of the star by a factor of 10 - 100 of initial radius of star. Therefore, the star becomes a giant or supergiant.

For systems in which the reaction preoducts escape the parameter $R$ was introduced; this is ratio of the energy realized in the hot gas to the energy supplied. Now the energy realized by the reraction appears as heat generated in the walls of apparatus, and thus has to be converted to electrical, mechanical or chemical energy before it can be fed back into the gas. If $\eta$ is the efficiency with which is can be done, then condition for a system with a net power gain is

$$\eta(R + 1) > 1. \quad (13)$$

The maximum value of $\eta$ is about 1/3, so what $R$ must be greater than 2 [3].

For the our pulsed cycle we have

$$R = \frac{tP_{reac}}{tP_B + 3nkT} = \frac{{P_{reac}}/{3n^2kT}}{{P_B}/{3n^2kT + {1}/{nt}}}, \quad (13\ a)$$

where $P_{reac}$ and $P_B$ are respectively the reacyion power and radiated p; ower per unite volume. The $3nkT$ term represents the energy required to heat the gas to a temperature $T$. Electron binding energies are neglected, but the contribution from electrons is included (this accounts for the factor 3 rather than 3/2) [3].

Since $P_{reac}$ and $P_B$ are are both proportional to $n^2$, $R$ is a function of the $T$ and $nt$. In Fig. 1 curves $R$ against $T$ for various values of $T$ for D – D reaction [3]

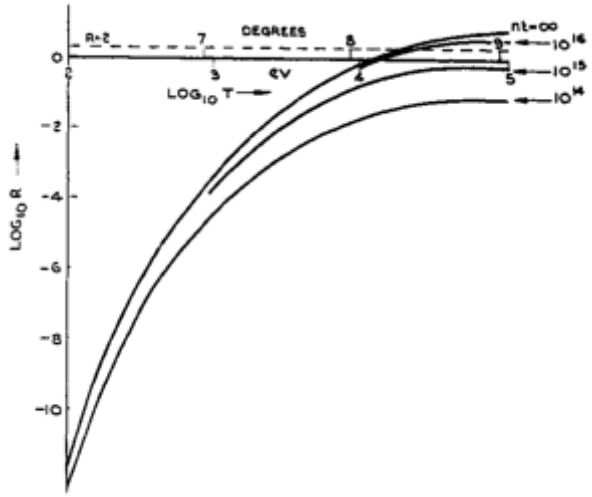


**Figure1.** *Variation of R with T for various values of nt for D – D reaction [3].*

Fig. 2 shows similar curvers for T- D reaction.

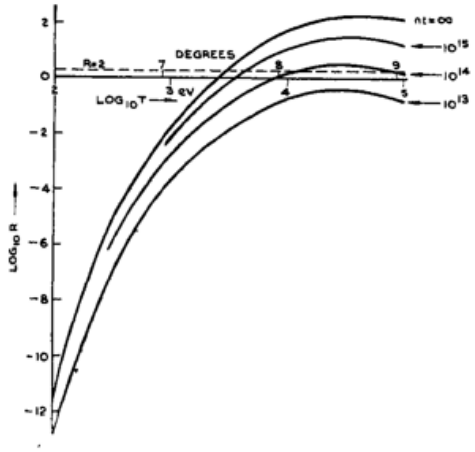


**Figure2.** *Variation of R with T for various values of nt for T – D reaction [3].*

### 2.3. Thomson – Benard phenomena

In the classical sense, the Thomson-Benard phenomenon consists in the formation of polygonal structures (most often hexagonal) during the transition from laminar to vortex motion of a liquid [6 -9], 24]. However, it can be used for other flows of matter, say electrons in semiconductors [24 -36].

Consider then a horizontal layer of fluid in which an adverse temperature gradient is maintained by heating the underside [7 -10, 24]. The temperature gradient thus maintained is qualified as adverse since, on account of thermal expansion, the fluid at the bottom will be lighter than the fluid at the top; and this is a top-heavy arrangement which is potentially unstable. Because of this latter instability there will be a tendency on the part of the fluid to redistribute itself and remedy the weakness in its arrangement. However, this natural tendency on the part of the fluid will be inhibited by its own viscosity. In other words, we expect that the adverse temperature gradient which is maintained must exceed a certain value before the instability can manifest itself.

The earlier experiments to demonstrate in a definitive manner the onset of thermal instability in fluids are those of Benard in 1900, though the phenomenon of thermal convection itself had been recognized earlier by count Rumford (1797) and James Thomson (1882) [8]. Further experiments were received by Benard and other researches. It will suffice to summarize here the principal facts established by them. They are: first, a certain critical adverse temperature gradient must be exceeded before instability can set in; and second, the motions which ensue on surpassing the critical temperature gradient have a stationary cellular character. What actually happens at the onset of instability is that the layer of fluid resolves itself into the number of cells; and if the experiment is performed with sufficient care, the cells

become equal and they align themselves to form a regular hexagonal pattern. Fig. 3 (which is a reproduction of one of Benard's early photograths) illustrates the phenomenon.

The theoretical foundations for a correct interpretation of the foregoing facts were laid by Lord Rayleygh in a fundamental paper [6]. Rayleygh showed that what decides the stability, or otherwise, of a layer fluid heated from below is the numerical value of the non-dimensional parameter, which was called larer Rayleygh number [7]

$$Ra = \frac{g\alpha\beta}{\kappa\nu} d^4, \tag{14}$$

where $g$ denotes the acceleration due to gravity, $d$ the depth of the layer, $\beta = \left|{}^{dT}/_{dz}\right|$ the uniform adverse temperature gradient which is maintained, and $\alpha, \beta$ and ν are the coefficients of volume expansion, thermometric conduictivity and kinematic viscosity, respectively.

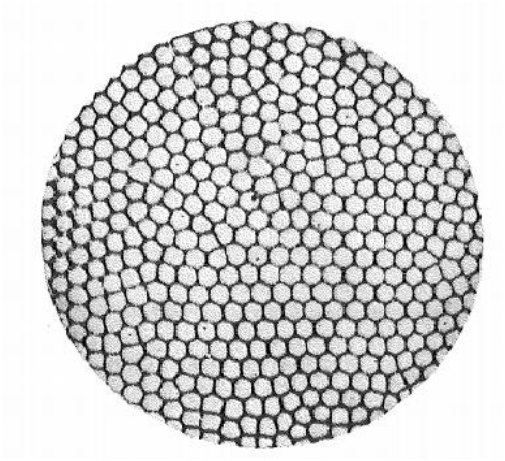

**Figure3.** *Benard cells in spermaceti [9].*

Rayleygh further showed that instability must set in when *Ra* exceeds a certain critical value $Ra_c$; and that when *Ra* just exceeds $Ra_c$, a stationary pattern of motions must come to prevail. The principal theoretical question is therefore: how is one to determine $Ra_c$?

For resolution of this problem system of equations of hydrodynamics (Euler and continuity) and thermo conductivity with corresponding boundary conditions were used.

Detail analysis of this problem is represented in [7, 24]. In this case, fluid flows were analyzed using hydrodynamic similarity criteria such as Rayleigh, Nusseldt, and Prandtl numbers.The instability of Rayleygh numbers for first even and first odd modes in Bussinesq approximation is represented in Fig. 4.

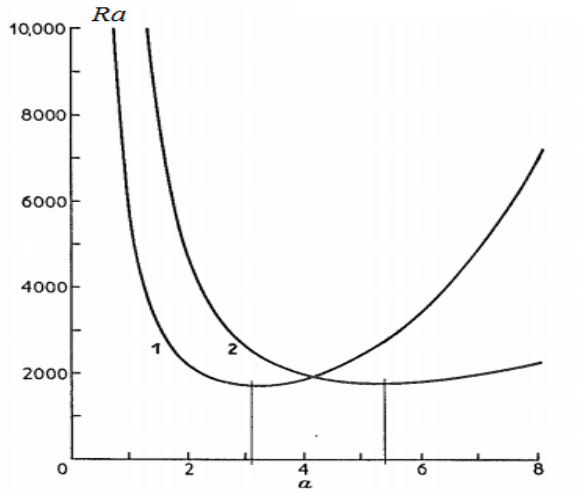


**Figure4.** *The Rayleygh number at which instablility sets in for disturbances of different wave numbers a for the first even (curve labeled 1) and the first odd (curve labeled 2) mode [7, 24].*

The proper solutions for тщкьфд тщву W (curve 1) and $(a^2Ra)^{-2/3}F$ (curve 2) for the state of marginal stability for the case when both bounding surfaces are rigid [7] are represented in Fig. 5. Where $F$ is $F(\infty, \Theta)$ [24].

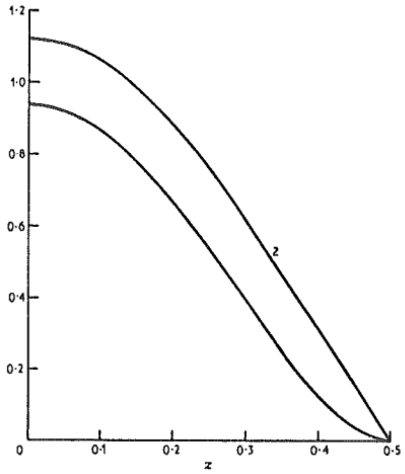


**Figure5.** *The proper solutions for W (curve 1) and $(a^2Ra)^{-2/3}F$ (curve 2) for the state of marginal stability for the case when both bounding surfaces are rigid [24].*

It is interesting to investigate whether it is possible to realize a somewhat similar situation in regard to the gas of charge carriers in a semiconductor [36]. Of course, here an electric field might play the role of the gravitational field. The reasons for posing this problem are clear: a periodic distribution of the electron temperature and (or) of the concentration of charge carriers (with a period exceeding the mean free path with respect to momentum) would imply that various macroscopic characteristics of the system are also periodically distributed, among them the electrical conductivity, the light absorption coefficient, etc. with obvious consequences [36]

### 2.4. Nonlinear optical phenomena and phase transitions

The processes of phase transitions and nonlinear optics are also related to critical phenomena. For the first time, H. Haken drew attention to the similarity of phase transitions of the 2nd kind and nonlinear optical phenomena [11, 12]. Later, this idea was developed in [27]. The processes of Quantum Electronics and Nonlinear Optics are equivalent to the processes of phase transition [11, 12]. But for the Nonlinear Optical phenomena these processes are nonequilibrium and acted at the time of generation of proper Nonlinear Optical effect.

We are represented a few examples of phase transitions in physical systems, eg in ferromagnets, were represented in [11]. Ferromagnet consists of a large number of elementary magnets were represented in [11]. If the temperature $T$ is greater than the "critical" temperature $T_c$, $T > T_c$, magnet axis oriented in random directions. If lower, then for $T = T_c$ the macroscopic number of elementary magnets suddenly builds up in one direction. Now ferromagnet characterized by spontaneous magnetization. Consideration solutions Fokker-Planck equations to set very close analogy between the phase transitions that occur in thermal equilibrium, and some transitions such order-disorder in nonequilibrium systems [11, 12].

As will be shown below, these transitions can occur in physics, chemistry, biology and other disciplines. To identify these analogies consider first the free energy $F$ of a system is in thermal equilibrium. The free energy $F$ is depended from the temperature $T$ and possibly on other parameters, such as volume. In this case we are searching the minimum free energy under some additional conditions. Their meaning is best explained by the example of a ferromagnet. If $M_1$ the elementary magnets aimed upward and $M_2$ elementary magnets facing downward, "magnetization" is

$$M = (M_{\uparrow} - M_{\downarrow})m, \tag{15}$$

where $m$ magnetic moment of one elementary magnet. Restriction is that the average magnetization $M$ must equal a given value

$$f_k = M. \tag{16}$$

As will be seen below, and other systems, we replace $M$ generalized coordinates $q$:

$$M \to q \text{ and } f_k = q. \tag{17}$$

In the future, a typical technique of L. Landau's theory of phase transitions is used.

H. Haken moves from thermodynamics to synergetics, nonlinear optical searches can also be represented as synergistic processes.

Represented above consideration should be taken with caution. We certainly can and will use the terminology associated with phase transitions. As will be shown below, this consideration can really apply to many non-equilibrium systems. But it must be said that the phase transitions in equilibrium systems Landau theory of phase transitions (Table 1) describes the phase transition incorrectly. In point of phase transition specific heat and other physical quantities have features that describe the so-called critical indices. Experimentally measured values of the critical parameters in the general case are not consistent with the predictions of the Landau theory. The main reason for this – inadequate consideration fluctuations. These phenomena are described successfully by Wilson's renormalization group [11, 12].

The analogy theory of phase transitions and synergetic is represented in Table 1 [11].

**Table3.1.** *The analogy with phase transition [11]*

| The physical system is in thermal equilibrium | Synergetic system that describes the stationary distribution function $f(q)$ |
|---|---|
| Order parameters $q$ | Order parameters $q$ |
| Distribution function $f = Nexp\left(-\frac{F}{kT}\right)$ | Distribution function $f(q) = \exp(-\hat{V})$, where $\hat{V} = lnf$ |
| Temperature | External parameters (increasing of energy) |
| Entropy | Action (decreasing of energy) |
| Specific heat | Changing actions by changing external parameters: efficiency |

This problem may be connected with L. de Broglie thermodynamics of point too [32].

The equivalence between ordered and disordered information may be represented with help de Broglie formula [32, 33], which is used in thermodynamics of point,

$$\frac{S_a}{\hbar} = \frac{S_e}{k_B}, \tag{18}$$

where $S_a$ – action, $S_e$– entropy, ħ – Planck's constant, $k_B$ – Boltzman constant.

This interpretation of the de Broglie ratio allows one to consider and analyze thermodynamic, deterministic and other informational processes and systems from a single point of view [33].

It should be noted that when describing Nonlinear Optical phenomena, it is advisable to use physico-chemical estimates, which sometimes more adequately describe the observed results. Thus, in the problem of self-focusing, there is a concept of the threshold energy of laser radiation, which is required for self-focusing - the "electrodynamic" formulas of Kelly and Marburger, which are calculated for Kerr media. These media include liquids and some solids. However, most solids are not Kerr media. Therefore, the following approach is more universal. It is known that classical nonlinear optical phenomena are caused by various impurities or local disturbances of the crystal lattice. The concentration of such impurities is $10^{14}$ - $10^{16}$ $cm^{-3}$ [23, 24]. In order to obtain the corresponding value, it is necessary to simply multiply the concentration of these impurities by their excitation energy, which leads to the corresponding nonlinear optical phenomenon. Such estimates coincide in order of magnitude with the estimates obtained using the Kelly and Marburger formulas [23, 24].

### 2.5. Cascade Model of Excitation of Chemical Bonds in the Regime of Saturation of Excitation

Main peculiarities of represented experimental data is showing its complexity. Roughly speaking we have trace of resulting interaction light and matter in irradiated matter.

In contrast to Nonlinear Optics, where we study the processes of interaction of light with matter as a change in radiation characteristics, in Relaxed Optics we study the processes of phase transformations of irradiated matter. It is obvious that we should investigate this problem from a physical-chemical point of view. Phase transformations of the irradiated material are due to changes in the structure of the irradiated material, that is, concentrations $10^{22}\ cm^{-3}$ [23, 34]. Therefore, we must search new methods of modeling.

The rough estimation of the energy characteristics of corresponding processes may be represent with help formula (19).

$$E_{ir} = \sum_i N_i \hbar\omega_i, \tag{19}$$

where $N_i$ is the concentration of proper centers of light scattering, $\hbar\omega_i$ is photon energy, $\hbar$ is Planck (Dirac) constant [23, 34].

For self-absorption the number of the scattering centers $N_i$ is equal the atom density the lattice $N_a$, which can be determined with help of next formula

$$N_a = \rho \frac{N_A}{A}. \tag{20}$$

Where $N_A$ – Avogadro number, $\rho$ – density of semiconductor, $A$ – a weight of one gram-atom or gram-molecule [23, 34].

We will analyze the experimental results on the formation of laser-induced donor centers in indium antimonide upon irradiation with nanosecond and millisecond pulses of a Ruby laser (wavelength 0,6943 $\mu m$, duration of pulse 20 *ns* and 5 – 6 *ms*) and series of nanosecond pulses of a neodymium laser (wavelength 1,024 $\mu m$, duration of pulse 10 *ns* and frequency of repetition 1 *kHz*) [23, 34, 35].

For indium antimonite $N_a \sim 4\cdot10^{21} cm^{-3}$. For more detail estimation of the results of *InSb* we are used the two-dimensional lattice (Fig. 6) [23, 34].

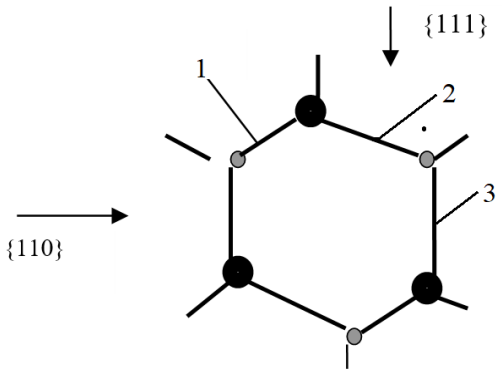


**Figure6.** *Two-dimensional picture the crystal lattice $A_3B_5$ (including InSb and InAs) the cubic symmetry (sphalerite). Bond 1 is pure covalent has energy 0.18 eV, bond 2 – 1.95 eV, bond 3 – 2.15 eV. [23, 34].*

Main estimations may be made with help modified formula (19)

$$E_{ir} = \sum_i N_a \varepsilon_{bi}. \tag{19 a}$$

Where $\varepsilon_{bi}$ is the energy of proper bonds from Fig. 6 (I =1, 2, 3). For InSb $\varepsilon_{b1} = 0.18\ eV$, $\varepsilon_{b2} = 1.95\ eV$, $\varepsilon_{b3} = 2.15\ eV$ [23, 34].

The breaking of bond 1 in the regime of saturation of excitation is corresponds to laser effect with optical pumping [23]. This effect has large differential photon efficiency, which can be determined with help formula (21)

$$n = 2\ln\frac{\hbar\omega_r}{E_g}, \tag{21}$$

where $\hbar\omega_r = 1.78\ eV$ for Ruby laser radiation, $E_g = 0.18\ eV$ and equaled of energy of bond 1. Crystals of indium antimonite in the sphalerite modification are direct-band, so the band gap corresponds to the minimum chemical bond energy. For *InSb* $n$ = 4.8. This fact ic caused grand relaxation time ~ $10^{-7}$ *s* for ruby laser irradiation[23, 34].

These data were using for the estimations of laser-induced damages (Rurherford backscattering spectra of protons with energy 500 *keV*) in *InSb* after 20 ns pulse Ruby-laser irradiation [23, 34]. Maximal value of Rutherford defectiveness is corresponding to value 0.1 $J/cm^2$. This value is correlating with receiving experimental data and corresponds to the breaking of bonds 1 and 2 in Fig. 2 [23, 34].

At the same time, one connection is the seed for other connections. Only in the mode of saturation of excitation of the previous connection (connections) do we have minimal energy expenditure to obtain the desired result.

Schema of Fig. 1 was using for the explanation the oriental effect of creation laser-induced n-centers in *InSb*. The angle between directions {111} and {110} is equal 37,5° for the bond 1 of Fig. 6. Therefore, coefficient of the anisotropy the the creation laser-induced centers is equal the square of the tangent of this angle – 0,45. Effective cross-section of absorption in {111} is more intensive as in direction {110} [23]. This is confirmed by experimental data upon irradiation with 20 *ns* pulses of a ruby laser [23].

The rupture of all three bonds leads to the appearance of a diffusion profile for 20 *ns* monopulse Ruby laser irradiation [23]. The estimates made according to formula (19 a) confirm our reasoning.

Form of profiles distribution of laser-induced doinor centerts was explained using the photokinetic model (adapted model of the phytoeffect). In the latter case, the difference in coefficients of laser-induced diffusion (self-diffusion) of indium and antimony atoms is assumed [23].

To estimate the life time of the corresponding processes, a phenomenological chain of relaxation times was constructed, which allows us to explain non-equilibrium and irreversible laser-induced processes from a single point of view [23, 34].

The experimental results which are receiving for *InSb* after irradiation millisecond pulse of Ruby laser and serie of nanosecond neodymium laser [35] can be explained in a similar way. Ruby laser irradiated milisecond profile (intensity of irradiation 5 $J/cm^2$) [344, 35] is simple to nanosecond profile (intensity of irradiation 0.1 $J/cm^2$) [34].

But the integral efficiency of transforming radiation into irreversible changes for the nanosecond regime of irradiation is larger by 2-3 orders of magnitude, as milisecond. This is explained by the fact that in the latter case, reradiation processes with photon energy of 0.18 *eV* play a major role. This is confirmed by the results of more complex profile of distribution of donor centers for Ruby pulse millisecond regiume of irradiation and nanosecond multipulse Neodimium laser irradiation. The shape of the profiles of these curves in the upper region corresponds to the absorption coefficient with a coefficient of $2 \cdot 10^5 cm^{-1}$ for ruby laser irradiation and $10^5$ $cm^{-1}$ for neodymium laser, the tail parts correspond to an absorption coefficient of the order of 100 $cm^{-1}$ of reradiation with a photon energy of 0.18 *eV*.

This means that a large contribution to the shapes of these profiles give the processes of reirradiation and reabsorption. The number of acts of reradiation can be estimated using formula (22) [23].

$$n = \frac{\tau_i I_{sat}}{\tau_r\left(1-\frac{\tau_r}{\tau_i}\right)I_0}. \qquad (22)$$

Where $\tau_i$ is time of irradiation, $\tau_r$ is rewlaxation time, $I_{sat}$ – the intensity of saturation of excitation (intensity 0.1 $J/cm^2$ nanosecond Ruby laser irradiation [34]) and $I_0$ – the intensity of irradiation. After substitution proper value of $I_{sat}$ and $I_0$ milisecond ruby lasser irradiation with 40 $J/cm^2$ [34, 35]we have $n \cong 10 \div 500$.

Experimental data [34] are certificated this hypothesis. Surface and volume concentrations donor centers in *InS*b after irradiation of nanosecond Ruby-laser pulses [34] is more in 3-4 orders as after millisecond irradiation [34, 35]. For this case we are using next model. The pa rt of absorbed irradiation with including process of *n*-reirradiation may be represented as

$$I_n = \frac{\frac{\tau_r}{\tau_i}}{1+\frac{\tau_r}{\tau_i}} I_0 e^{-\alpha x}. \qquad (23)$$

For this case we have $\frac{\tau_r}{\tau_i} = 0.05 - 0.1$. For Ruby laser irradiation [23, 34] we can determine relaxation time $\tau_r = (0.05 - 0.1)\tau_i = (0.25 - 0.5)ms$.

For estimation the efficiency of generation n-centers for the nanosecond [34] and millisecond [35] regimes of irradiation we used next formula.

$$\beta = \frac{I_{sat}/N_{avsat}}{I_{ir}/N_{avir}}. \quad (24)$$

This formula give next values: $2.5 \cdot 10^{-6}$ for subsurface part Ruby milisecond profile (intensity of irradiation 40 J/cm$^2$) and $2.5 \cdot 10^{-7}$ for tail part. For Ruby milisecond profile (intensity of irradiation 5 *J/cm*$^2$) this efficiency is equaled $2 \cdot 10^{-6}$. For Ruby nanosecond profile (intensity of irradiation 0.1 *J/cm*$^2$) photon effgiciency is equaled ~ 0.5 – 0.8. Therefore, processes of reirradiation may be used for the formation more deep parts of irradiated matter [23, 34].

Thus, the model based on Fig. 6 makes it possible to explain the main regularities of changes in electrophysical characteristics of irradiated antimonide and indium arsenide, but does not allow evaluating laser-induced structural changes.

Now we show the using of cascade model for the explanation experimental data of laser-induced surface physical-chemical phase transformations in silicon and germanium [15, 16, 24, 26, 34].

However, it is possible to build a model that allows you to estimate laser-induced structural changes in irradiated materials. Thus, to explain the experimental results for generation of laser-induced surface and subsurface structures of *Si* [15, 16, 26] and *Ge* [23, 24], a physico-chemical model was built based on the phase diagram of silicon (Fig. 8) [17].

It can be seen from this figure that silicon (by analogy with germanium) has four crystallographic modifications, and taking into account quasi-crystalline modifications – twelve [23, 24]. We will dwell only on crystallographic modifications.

To determine the energy that falls on one coordination or layer, we will use the Seitz energy definition from the radiation physics of a solid body [30]. This energy of the silicon is equal to 12.6 *eV*, and the number of nearest neighbors is equal to the coordination number. In addition, in the diamond lattice, all bonds are covalent and equal to each other. We know that one coordination number in silicon corresponds to an energy of 1.6 *eV*. For germanium - 1.3 *eV* for similar reasons. By the way, this energy is equal to the energy of the corresponding covalent bonds by L. Pauling [23, 24, 34]. Next, if we multiply the value of this energy by the density of atoms of the corresponding lattice and by the difference in the corresponding coordination numbers, we will obtain the corresponding value of the transition energy from one crystallographic modification to another.

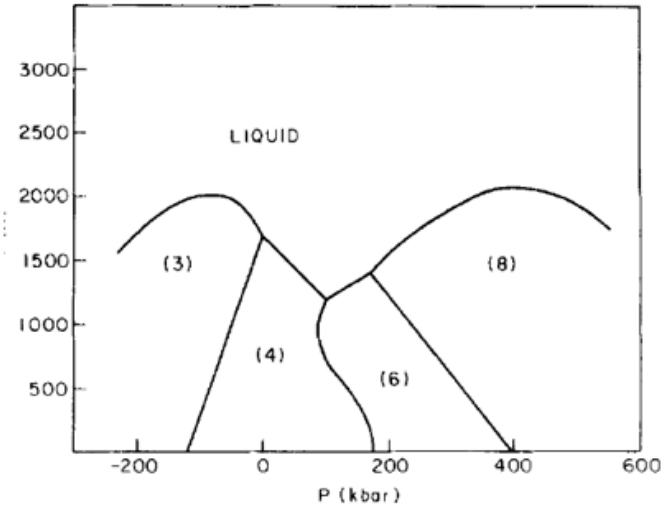


**Figure7.** *A schematic phase diagram for Si(CN). The coordination numbers (CN) of the various phases are indicated. The diagram is based on common features of the phase diagrams of column IV elements as described by the references cited in Pistorius's review [18]. Starting from a high temperature >3·10$^3$K and subject to a constraint of average density* $\langle\rho\rangle = \rho(4)$*, a hot micronucleus will tend to bifurcate into the most stable phases (highest* $T_m$*) which straddle Si(4) in density. These are Si(3) and Si(8), as indicated by the diagram [17].*

Let initial crystal semiconductors *Si* and *Ge* have, the diamond structure.

We have from formula (20) for *Si* $N_{aSi} = 5 \cdot 10^{22} cm^{-3}$, and for *Ge* $N_{aGe} = 4.4 \cdot 10^{22} cm^{-3}$. Please, leave two blank lines between successive sections as here. However, *Si* and *Ge* may be crystallizing in lattices with hexagonal, cubic, trigonal and monoclinic symmetry [23, 24, 34].

Coordination number (CN) 8 is corresponded of diamond lattice, CN 6 – hexagonal lattice, (CN) 4 and (CN) 3 – other two lattices. It should be noted that melting temperatures of these phases are various. Volume density of CN is equaled $CN \cdot N_a$. For diamond symmetry of lattice, this value is $8N_a$ [24].

We can determine corresponding volume density of energy, which is necessary for transition between proper crystal structures with help formula (19 a).These data are represented in Table 2 [24].

**Table2.** *Volume density of energy $I_{vi}$ ($10^3$ J/cm$^3$), which is necessary for the breakage of proper coordination numbers (CN) in the regime of saturation of excitation in Si and Ge [24].*

| | $I_{v1}$ | $I_{v2}$ | $I_{v4}$ | $I_{v5}$ |
|---|---|---|---|---|
| Si | 12.8 | 25.6 | 51.2 | 64 |
| Ge | 7.6 | 15.1 | 30.2 | 37.8 |

To obtain the surface density of irradiation energy, we must divide the value given in Table2 by the corresponding light absorption index. These results are analyzing in [23, 24]. As in the case of indium antimonide, differential photon efficiency (light absorption conditions) is crucial for silicon. This explains why the efficiency of formation of microstructures by nanosecond pulses of an excimer laser (photon energy of 4.25 *eV*, pulse duration 25 *ns*) [15, 16] is greater than by femtosecond laser pulses (photon energy of 1.51 *eV*, pulse duration 130 *fs*) [26]. In both cases, hedgehog-like structures are formed, and the "needles" of structures of lower symmetry are perpendicular to the surface of previous structures with higher symmetry [15, 16, 26].

### 2.6. Laser-Induced Optical Break Down and Shork Processes

Now we represent cascade model of optical lasser-induced breakdown [25, 28, 29]. This model allow to explain experimental data of laser induced optical breakdown in SiC (duration of pulse 130 *fs*, wavelength 800 *nm*, intensity of irradiation 200 – 300 *nJ*/*pulse*, $TEM_{00}$ mode) [18, 19] and in KCl (duration of pulse 30 *ns*, wavelength 10.6 *μm*, intensity of irradiation 2 *J*/*pulse*, $TEM_{01}$ mode) [22]. Let us now turn to the explanation of the experimental results of the optical analysis of silicon carbide [18, 19] and potassium chloride [22].

That is why a cascade model was proposed, which is based on the transformation of the initial exposure and the creation of non-uniform exposure of the material [25, 28, 29]. This cascade is including diffraction stratification of focused radiation, generation of conical Cherenkov radiation, interference of the short-wavelength part of Cherenkov radiation, and actual optical breakdown in the maxima of the interferogram [25, 28, 29].

Diffraction stratification and generation of surface Cherenkov radiation belong to the first [25]. The second group includes optical breakdown, including the formation of nanovoids [25].

Diffraction stratification was modeling with help of Rayleygh rings concept [25, 28, 29].

Cherenkov radiation may be certified with macroscopic and microscopic ways [9, 10].

The Golub macroscopic [21] and A. Bohr [20] microscopic mechanisms of Cherenkov radiation were synthesizing with help of next formula [25, 28, 29].

$$\theta_{ch} + \alpha_{ir} = {}^{\pi}/_{2} \text{ or } \theta_{ch} = {}^{\pi}/_{2} - \alpha_{ir}, \quad (25)$$

Where $\theta_{ch}$ – Cherenkov angle, $\alpha_{ir}$– angle between tangent line and direction of laser beam.

Angle $\alpha_{ir}$ was determined from next formula [25]

$$tan\alpha_{ir} = {}^{d_b}/_{l_f}, \quad (26)$$

where $d_b$ – diameter of laser beam, $l_f$ – length of focusing or self-focusing. In our case $\alpha_{ir}$ is angle of focusing or self-focusing.

This formula is approximate for average angle $\alpha_{ir}$.

Golub formula for case of nonlinear polarization has next kind [21]

$$cos\theta_{Ch}=\frac{c}{n_2(\omega)v_{nlpol}}, \quad (27)$$

where $(\omega)$ is nonlinear refraction index, $v_{nlpol}$ is velocity of generation of nonlinear polarization.

The proper foci The Golub formula (27) was using for the determination of corresponding order of diffraction ring may be determined with help next formula [25, 34]

$$l_{nf} = \frac{d_{ndif}}{2\tan^{\varphi}/_{2}}. \quad (28)$$

According to [18, 19] we have five diffraction rings. Each surface of cone this diffraction stratification is source of Cherenkov radiation. This is confirmed by experimental facts that supercontinuum (Cherenkov) radiation has a surface character [25, 28, 29, 34].

The estimation of energy distribution in five Mach cones was made by next formula [25, 34]

$$E_{1ob} = \frac{\pi^2}{4}\left(\sum_{i=1}^{5} n_{iav}^2\, l_{iav}\right)r^2 N_{aSiC}E_{Zth}, \quad (29)$$

where $n_{iav}$– average visible number of filaments in proper group of cascade, $l_{iav}$=1000 *nm* – average length of filaments in proper group of cascade, $r$ = 10 *nm* – average radius of filament, $N_a$ – atom density of 4H-*SiC* [25, 34].

The atom density of 4H-*SiC* may be determined with help formula (20). For 4H-*SiC* $N_{aSiC} = 9.4 \cdot 10^{21} cm^{-3}$.

Energy, which is necessary for the optical breakdown our nanotubes may be determined in next way. Zeitz threshold energy for 4H-*SiC* is equaled $E_{Zth}$ ~ 25 *eV* [30]. Let this value is corresponded to energy of optical breakdown. Therefore, summary energy $E_{1ob}$ is equaled

$$E_{1ob} = N_{asnt} \cdot E_{Zth} = 23.2\ nJ. \quad (30)$$

This value is equaled of ~ 8% from pulse energy or ~ 30% from the effective absorbed energy of pulse [25, 34]. As we can see, Cherenkov radiation generates laser radiation more effectively than charged particles or gamma radiation.

If this scenario is true, we have as for 4H-SiC effective transformation the energy of laser radiation to cascade of laser-induced breakdown for *KCl* too. I n this case ve have 7 double cascade which is ccorresponde to $TEM_{01}$ mode of laser radiation [22]. This value is 11,6 – 17,4 percents [25, 34].

The sizes of nanovoids [19] may be determined with help modified Rayleygh model [25, 34] and its form – the help methods of continuum mechanics [25, 28, 29, 34]] in next way.

For the estimations of maximal radius of nanovoids we must use modified Rayleygh formula [10, 25, 34]

$$R_{max} = \frac{2R}{0.915r}\sqrt{\frac{E_{ir}}{\pi\tau_{ir}cE}}, \quad (31)$$

where $T_c$ – the time of creation the nanovoid (bubble), $R$ is radius of nanovoid, $r$ – radius of irradiated zone, $E$ – Young module, $E_{ir}$– energy of one pulse. $\tau_{ir}$ – duration of pulse.

If we substitute $r$ = 250 *nm*, $R$ = 10 *nm*, $E$ = 600 *GPa* [25, 34], $E_{ir}$=300 *nJ*, $\tau_{ir}$ = 130 *ps*, $c$=3·10$^8$ *m/s*, than have $R_{max}$=11 *nm.*

The velocity of shock waves for femtosecond regime of irradiation is less as velocity of sound. However, we have two velocities of sound in elastic body: longitudinal $v_{ls}$ and transversal $v_{ts}$ [25, 28, 29, 34]. Its values are determined with next formulas

$$v_{ls} = \sqrt{\frac{E(1-\nu)}{\rho_0(1+\nu)(1-2\nu)}}, \text{ and } v_{ts} = \sqrt{\frac{E}{\rho_0(1+\nu)}} \quad (32)$$

where $\nu$ – Poisson's ratio [25, 34]. The ratio between of these two speeds is equaled

$$\alpha = \frac{v_{ts}}{v_{ls}} = \sqrt{\frac{(1-2\nu)}{2(1-\nu)}}. \quad (33)$$

However, this ratio must be true for shock waves too. Therefore, for silicon carbide for $\nu$ = 0,45 [25, 34] $\alpha$ = 0,33. Roughly speaking last ratio is determined the step of ellipsoidal forms of our nanovoids [19].

In this case, we represented 4H-SiC as isotropic plastic body. For real picture, we must represent hexagonal structure. However, for the qualitative explanation of experimental data *KCl* [22] this modified Rayleygh model allow explaining and estimating the sizes and forms of receiving nanovoids [25, 34].

We can estimate sizes and forms of possible nanovoids for potassium chloride too. Let's take the ratio of the radius of the irradiation zone to the radius of the nanowire as 50. The energy of irradiation is 2 *J*. The duration of irradiation is 50 *ns*. Young's modulus 29.67 *GPa*, Poisson's ratio 0.216 [25, 34].

After substitution, these data to formula (31) we have $R_{maxKCl} = 62.5nm$. Ellipticity of *KCl* nanovoids may be determined from (33) $\alpha_{KCl} = 0.6$.

Let us now estimate the maximum bubble radii for the acoustic case. For this, in formula (31), you need to change the speed of light to the speed of sound (31 a).

$$R_{max}^{ac} = \frac{2R}{0.915r}\sqrt{\frac{E_{ir}}{\pi\tau_{ir}c_sE}}, \quad (31\ a)$$

where $c_s$ is speed of sound.

As a result, we get $R_{maxSiC}^{ac} = 1.7\mu m$ and $R_{maxKCl}^{ac} = 28\mu m$. The shape of the voids does not change, they just increase in size by 2-3 orders of magnitude [25, 34].

If we take the ratio of the acoustic formula (31 a) and the optical formula (31), then for the same irradiation modes we have the ratio

$$\frac{R_{max}^{ac}}{R_{max}} = \sqrt{\frac{c}{c_s}}. \quad (34)$$

However, a comparison with the experimental results [18, 19, 22] shows those electromagnetic rather than acoustic processes play the main role in the formation of nanovoids. This is explaining by the fact that in this case a chain of close-range coherent processes of transformation of both optical radiation into the excitation of the medium and the corresponding relaxation of the medium is implemented, in other words, there is a chain of interconnected coherent transformations.

## 3. Conclusions

1. Main peculiarities of formulation main criteria and principles in theory of critical phenomena and processes are observed.
2. Two Veinberg-Vigner teorems in nuclear reactor theory as critical principles are represented.
3. Thermonuclear problems are researched on the basis Lawson criterion (pulse processes) and Schönberg-Chandrasekar evolutionary limit (star stationary processes) are discussed.
4. Thomson-Benard phenomena is observed as transition from stationary to curl flows in hydrodynamics and electrons.
5. Formal analogy between second-order phase transitions and nonlinear optical processes is analysed with help H. Haken synergetic method and generalizing de Broglie formula.
6. Cascade model of excitation selected types and number of chemicalas bonds are analyzed for InSb and InAs (two-dimensional lattice) and for silicon and germaium (phase diagram).
7. Csascade model of laser-induced optical breakdown for focused pulse laser irradiation is shown the influence the transformation of optical radiation (diffraction stratification, Cherenkov radiation and interference lowwave part of this Cherenkov radiation).
8. Comparative analysis of other properties of acoustic and electromagnetic chock processes in SiC and KCl is representing too.

## REFERENCES


[1]. Weigner A. M., Wigner E. P. (1959) The Physical Theory of Neutron Chain Reactors. University Press, Chicago

[2]. Shirokov S. V. (2011) Physics of Nuclear Reactors. Vysheyshaya Shkola, Minsk (In Russian)

[3]. Lawson J. D. (1957) Some Criteria for thr bPower Producing Thermonuclear Reactor. Proc. Of the Physical Society, Sec. B, 70(1), 6-10.

[4]. Andrievsky S. M., Klymyshyn I. A. (2007) General astronomy course. Astroprint, Odessa (In Ukrainian)

[5]. Schönberg M., Chandrasekar S. (1942) On the evolution of main-sequence star. The Astrophysical Journal, Vol. 96, Is.2, 161-172.

[6]. Rayleygh (J. W. Strutt) (1916) On convective currents in a horizontal layer of fluid then the higher temperature is on the under side. Philosoph. Mag., Vol. 32, 529-546.

[7]. Chandrasekar S. (1981) Hydrodynamic and Hydromagnetic Stability. Dover Publications, New York.

[8]. Thomson J. (1882) On a changing tesselated structure in certain liquids. Proceedings of the Philosophical Society of Glasgow. Vol. 8, Is. 2, 464–468.

[9]. Bénard Henri (1900) Les tourbillons cellulaires dans une nappe liquide. Revue Générale des Sciences Pures et Appliquées. Vol. 11, – P.1261–1271, 1309–1328 (in French)

[10]. Rayleygh (J. W. Strutt) (1917) On the pressure developed in a Liquid during the Collapse of a Spherical Cavity. The London, Edinburgh and Dublin Philosophical Magazine and Journal of Science. Vol. 34, 94-98.

[11]. Haken H. (1977) Synergetics: An Introduction Nonequilibrium Phase Transitions and Self-Organization in Physics, Chemistry and Biology. Springer Verlag, Berlin.

[12]. Perina J. (1991) Quantum statistics of linear and nonlinear optical phenomena. 2-d ed. Kluwer, Dordrecht

[13]. Haken H. (1981) Light, Vol. 2: Laser Light Dynamics. North Holland, Amsterdam\

[14]. Wayne R. P. (1988) Principles and Applications of Photochemistry. University Press, Oxford

[15]. Pedraza A. J., Fowlkes J. D. and Lowndes D. H. (1999) Silicon microcolumn arrays growth by nanosecond pulse laser irradiation. Appl. Phys. Lett. 74(10), 2222-2224.

[16]. Pedraza A. J., Guan Y. F., Fowlkes J. D., Smith D. A. and Lowndes D. H. (2004)Nanostructures produced by ultraviolet laser irradiation of silicon. I. Rippled structures. J. Vac. Sc. @ Techn. B., vol. 22, no.10, 2823-2835.

[17]. Philips J.C. (1981) Metastable honeycomb model of laser annealing.//Journal of Applied Physics, No.12, Vol. 52, 7397–7402

[18]. Okada T., Tomita T., Matsuo S., Hashimoto S., Ishida Y., Kiyama S., Takahashi T. (2009) Formation of periodic strain layers associated with nanovoids inside a silicon carbide single crystal induced by femtosecond laser irradiation. J. Appl. Phys., v. 106, p.054307, 5 p.

[19]. Okada T., Tomita T., Matsuo S., Hashimoto S., Kashino R., Ito T. (2012) Formation of nanovoids in femtosecond laser irradiated single crystal silicon carbide. Material Science Forum , vol. 725, 19 – 22.

[20]. Bohr A. (1948) Atomic interaction in penetration phenomena. Der KGL Danske Videscabernes Selskab. Matematisk-Fysiske Meddelelser, Bind 24, Nr. 190, 1-52.

[21]. Golub I. (1990) Optical characteristics of supercontinuum generation. Optics Letters. Vol. 15, Is.6, 305-307

[22]. Yablonovich E. (1971) Optical Dielectric Srength of AlkaliHalide Crystalls Obtained by Laserinduced Breakdown. Appl. Phys. Lett., vol.19, is.11, 495-497.

[23]. Trokhimchuck P. P. (2020) Relaxed Optics: Modelling and Discussions. Lambert Academic Press, Saarbrukken

[24]. Trokhimchuck P. P. (2022) Relaxed Optics: Modelling and Discussions 2. Lambert Academic Press, Saarbrukken

[25]. Trokhimchuck P. P. (2024) Relaxed Optics: Modelling and Discussions 3. Lambert Academic Press, Saarbrukken

[26]. Shen M., Carey J. E., Crouch C. H., Kandyla M., Stone H. A., Mazur E. (2008) High-density regular arrays of nano-scale rods formed on silicon surfaces via femtosecond laser irradiation in water.// Nanoletters, vol. 8, is. 7, 2087-2091.

[27]. Andreev A.V., Emelyanov V.I., Il'ynskiy Yu.A. (1988) Cooperative phenomena in optics. Nauka, Moscow (In Russian)

[28]. Trokhimchuck P. P. (2020) Some Problems of the Modeling the Optical Breakdown and Shock Processes in Nonlinear and Relaxed Optics, IJARPS, Vol. 7, Is.5, 17-30.

[29]. Trokhimchuck P. P. (2023) Shork Electromagnetic Processes in Nonlinear and Relaxed Optics. In: Recent

Review and Research in Physics. Ed. Jayminkumar Rajanikant Ray, S.S. Sharma, Vol. 4, ch.3. New Delhi: AkiNik Publications, 23-52.

[30]. Trokhimchuck P. P. (2007) Radiation Physics of Status Solid, Vezha, Lutsk (In Ukrainian)

[31]. Bourne N. K. (2001) On the laser ignition and initiation of explosives. Proc. Roy. Soc. London A. Vol. 457, 1401-1426.

[32]. De Broglie L. (1964) Thermodynamics of isolated point (Hidden thermodynamics of particles). Gauthiers Villars, Paris (In French)

[33]. Trokhimchuck P. (2024) Main Problems of Unification the Basic Laws of Physics and Information Theory. International Journal of Physics and Mathematics, vol. 6, is.1, 39-45.

[34]. Trokhimchuck P. (2024) Some problems of modelling the physical-chemical processes in Relaxed Optics. AIP Conference Proceedings 3084 (1), 10 p.

[35]. Bogatyryov V.A., Kachurin G.A. (1977) The creation low resistively n-layers on *InSb* with help the impulse laser irradiation. Physics and technical of semiconductors, v.11, No.1, 100-102. (In Russian)

[36]. Bonch-Bruevich V. L. (1975) The Benard problems for hot electrons in semiconductors.// Sov. Phys, JETP. Vol. 40, No. 6, 1092-1098. (In Russian)

**Citation:** *Petro P. Trokhimchuck. " To Question about Main Principles and Criteria of Critical Processes and Phenomena" International Journal of Advanced Research in Physical Science (IJARPS), Vol 11, issue 06, pp. 1-17., 2024.*